

Electronic Supplementary Information

**Expression of biocatalysts and their use in monomer synthesis  
for biodegradable polymer from acetone and CO<sub>2</sub>**

Yu Kita,<sup>a</sup> Ritsuko Fujii<sup>a,b</sup> and Yutaka Amao<sup>\*a,b</sup>

a. Graduate School of Science, Osaka City University, 3-3-138 Sugimoto, Sumiyoshi-ku, Osaka 558-8585, Japan

b. Research Centre for Artificial Photosynthesis (ReCAP), Osaka Metropolitan University, 3-3-138 Sugimoto, Sumiyoshi-ku, Osaka 558-8585, Japan

E-mail: amao@omu.ac.jp

## Table of Contents for Supporting Information

Experimental method of PMF analysis.....	3
Table. S1. The elements of RCVB medium.....	3
Figs. S1 - S2. Detection for acetoacetate using ion chromatography.....	4, 5
Figs. S3 - S4. Detection for $\beta$ -hydroxybutyrate using ion chromatography.....	5, 6
Figs. S5. The amino acid sequence of AC and HBDH from <i>Rb. Capsulatus</i> SB1003.....	7
Fig. S6. The MALDI-TOF mass spectrum of apparent molecular masses of 87.1 kDa of the electrophoretic gel.....	8
Fig. S7. The MALDI-TOF mass spectrum of apparent molecular masses of 79.0 kDa of the electrophoretic gel.....	9
Fig. S8. The MALDI-TOF mass spectrum of apparent molecular masses of 21.3 kDa of the electrophoretic gel.....	10
Fig. S9. The MALDI-TOF mass spectrum of apparent molecular masses of 26.8 kDa of the electrophoretic gel.....	11
Fig. S10. The MALDI-TOF mass spectrum of apparent molecular masses of 24.6 kDa of the electrophoretic gel.....	11
Fig. S11. Time course of the ion chromatogram for acetoacetate production with AC.....	12
Fig. S12. Time course of the ion chromatogram for acetoacetate production with AC under various $Mg^{2+}$ concentrations.....	13
Fig. S13. Time course of the ion chromatogram for acetoacetate production with AC under various pH.....	14
Fig. S14. Effect of $Mg^{2+}$ on HBDH for acetoacetate reduction to $\beta$ -hydroxybutyrate.....	15
Fig. S15. Time course of ion chromatogram for one-pot $\beta$ -hydroxybutyrate synthesis with AC and HBDH.....	16
Fig. S16. Time course of ion chromatogram for one-pot $\beta$ -hydroxybutyrate synthesis with AC and HBDH under pH 8.2.....	16
Figs. S17 – S19. Determination of stereospecificity of HBDH in the cell extract.....	17, 18, 19
Fig. S20 Determination of optical isomer of $\beta$ -hydroxybutyrate synthesized in a one-pot.....	20

### Experimental method of PMF analysis

The gel spots were excised and in-gel digestion with trypsin (Sequencing Grade Modified Trypsin, V6111, Promega Co., WI, USA) was performed by DigestPro 96 (CEM Japan K.K., Tokyo). The supernatant was collected and desalted using the C18-ZipTip (Millipore). MALDI mass spectrometry was performed using a Bruker Autoflex Speed TOF/TOF mass spectrometer (Bruker) in positive ion mode with  $\alpha$ -cyano-4-hydroxycinnamic acid (CHCA) as the matrix in the m/z range from 800 to 4000. After deconvolution, the MS peaks were applied to peptide fingerprinting analyses against the concerned four sequences (Accession numbers of GenBank are ADE85085.1, ADE85084.1, ADE85086.1, and ADE85562.1, for  $\alpha$ -,  $\beta$ -, and  $\gamma$ -subunits of AC and HBDH, respectively) using Biotoools ver 3.2 software (Bruker) with a matching threshold of less than 50 ppm.

Table. S1. The elements of RCVB medium

10% DL-malate	40 mL	**Trace elements	
10% (NH <sub>4</sub> ) <sub>2</sub> SO <sub>4</sub>	10 mL	Na <sub>2</sub> EDTA	2.5 g
0.64 M KPO <sub>4</sub>	15 mL	CoCl <sub>2</sub> · 6H <sub>2</sub> O	0.02 g
150 µg/mL (+)-Biotin	0.1 mL	MnCl <sub>2</sub> · 4H <sub>2</sub> O	0.2 g
*Super salts solution	50 mL	H <sub>3</sub> BO <sub>3</sub>	0.1 g
Ultrapure water	to 1 L	CuCl <sub>2</sub> · 2H <sub>2</sub> O	0.01 g
		ZnCl <sub>2</sub>	0.05 g
		Na <sub>2</sub> MoO <sub>4</sub> · 2H <sub>2</sub> O	0.1 g
*Super Salts solution		NiCl <sub>2</sub> · 6H <sub>2</sub> O	0.05 g
1.0% Na <sub>2</sub> EDTA	20 mL	Na <sub>2</sub> SeO <sub>3</sub>	0.005 g
20% MgSO <sub>4</sub> · 7H <sub>2</sub> O	10 mL	NaVO <sub>3</sub>	0.005 g
7.5% CaCl <sub>2</sub> · 2H <sub>2</sub> O	10 mL	Ultrapure water	to 0.5 L
0.5% FeSO <sub>4</sub> · 7H <sub>2</sub> O	24 mL		
1.0g/L thiamine-HCl	1 mL		
**Trace elements	10 mL		
Ultrapure water	to 1 L		

### Detection for acetoacetate using ion chromatograph

The amount of acetoacetate was detected using ion chromatography system (Metrohm, Eco IC; electrical conductivity detector) with an ion exclusion column (Metrosep Organic Acids 250/7.8 Metrohm; column size: 7.8 x 250 mm; composed of 9  $\mu\text{m}$  polystyrene-divinylbenzene copolymer with sulfonic acid groups). The 1.0 mM perchloric acid and 50 mM lithium chloride in aqueous solution were used as an eluent and a regenerant, respectively. Flow rate of eluent solution was adjusted to be  $0.5 \text{ mL min}^{-1}$ . The retention time for acetoacetate was detected at 13.5 - 14.5 min. The electrical conductivity changes in the various acetoacetate concentrations (100 - 1000  $\mu\text{M}$ ) were shown in Fig. S1.

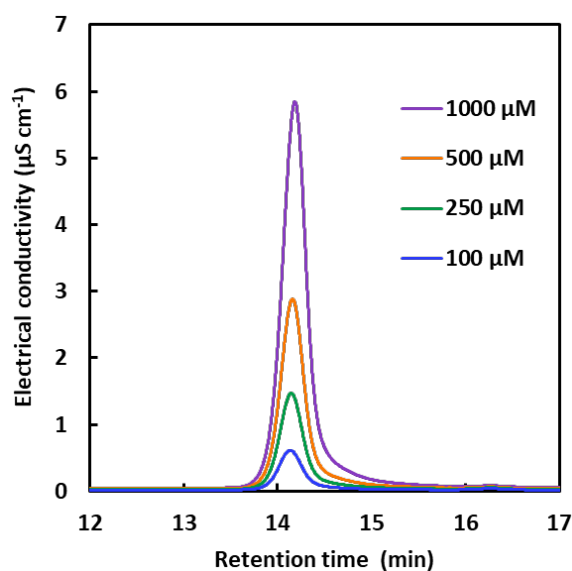


Fig. S1. Chromatogram of lithium acetoacetate (100 – 1000  $\mu\text{M}$ ) in 50 mM HEPES buffer (pH 7.0).

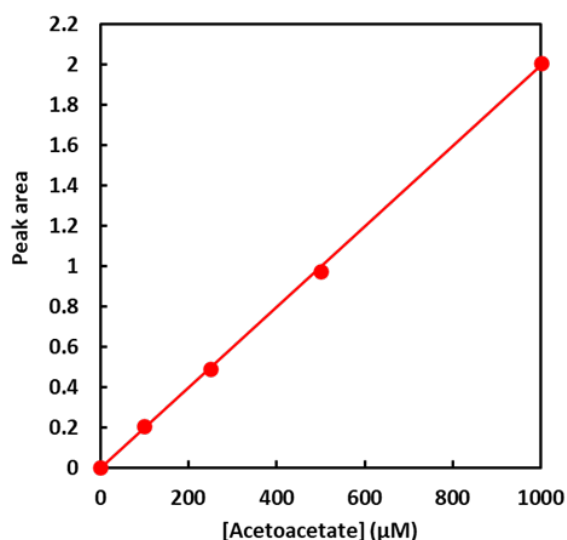


Fig. S2. Relationship between the acetoacetate concentration and the detection peak area.

As shown in Fig. S2, the acetoacetate concentration and the detected peak area showed a good linear relationship (correlation coefficient:  $r^2=0.999$ ) as following equation (S1).

$$\text{Peak area} = 0.0020 \times [\text{Acetoacetate}] (\mu\text{M}) \quad (\text{S1})$$

#### Detection for $\beta$ -hydroxybutyrate using ion chromatograph

The amount of  $\beta$ -hydroxybutyrate was detected using ion chromatography system (Metrohm, Eco IC; electrical conductivity detector) under the same conditions as acetoacetate detection. The retention time for  $\beta$ -hydroxybutyrate was detected at 14.2 - 15.2 min. The electrical conductivity changes in the various  $\beta$ -hydroxybutyrate concentrations (100 - 1000  $\mu\text{M}$ ) were shown in Fig. S3.

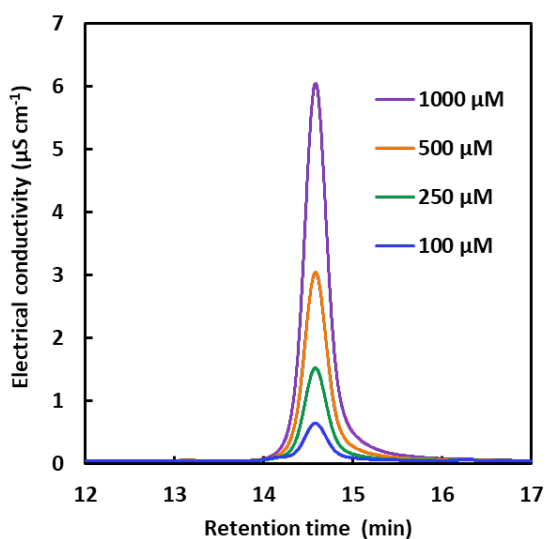


Fig. S3. Chromatogram of sodium  $\beta$ -hydroxybutyrate (100 - 1000  $\mu\text{M}$ ) in 50 mM HEPES buffer (pH 7.0).

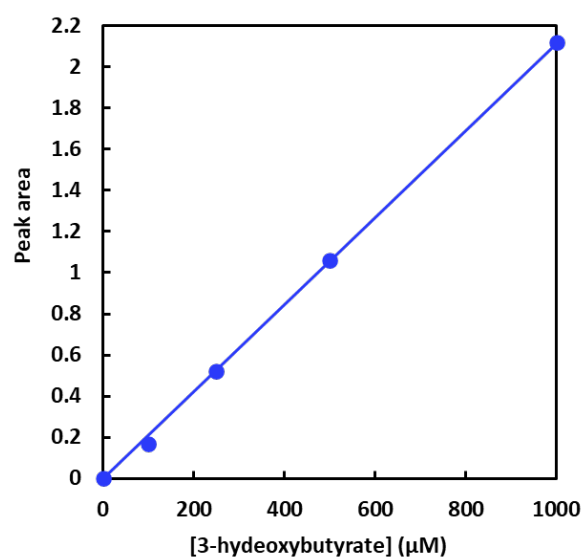


Fig. S4. Relationship between the  $\beta$ -hydroxybutyrate concentration and the detection peak area.

As shown in Fig. S4, the  $\beta$ -hydroxybutyrate concentration and the detected peak area showed a good linear relationship (correlation coefficient:  $r^2=0.999$ ) as following equation (S2).

$$\text{Peak area} = 0.0021 \times [\beta\text{-hydroxybutyrate}] (\mu\text{M}) \quad (\text{S2})$$

(a)  $\alpha$  subunit of AC from *Rb. capsulatus* SB1003

```
MNAPTAIRGIVRGGDTLKQHRDGIMEASKRTGHYAGLKQMELRDSDPIMYNKLFSLRAGVVDARETAKK
IAASPIVEQEGELCFTLYNAAGDSILTSTGIIHVGTMGAAIKYMIENDWESNPGVKDRDIFCNNDSLIG
NVHPCDIHTIVPIFHEGELIGWVGGVTHVIDTGAVGPGSMTTGQVQRFGDGYSVTCRKGENDTLFRDWL
HESQRSVRTTRYWMLDERTRIAGCHMIRKLVAEVIAEEGIEAYWKFAYEAVEHGRLGLQNRKAMTIPGK
YRQVGFVDVPYAHDDVVRVPSDFAKVDTIMHTPSEMTIRPDGTWRLDFEGASRWGWHTYNAHSVSFTSGIW
VMMTQTLIPTEMINDGAAAYGTEFRLPKGTWMNPDDRRVAFAYSWHFLVSSWTALWRGLRSYFGRGYLEE
VNAGNANTSNLQGGGFNQYDEIHAVNSFECAANGVGASAIGDGLSHAAAIWNPEGDMGDMEIWELAEPL
VYLGRQIKASSGGAGKYRGGCGFESLRMVWNAKDWTFMFMGNHISDGLMGGYPAASGYRFEAHETGLKEII
AQGGDIPHGGDTPGNPVDGLLKGARIKRDQKAITTEAMFKDYDLYLNYMRGGPGFGDPLDRDPG
AVAADVNGGYLVERFAQSVYGVVLVKGADGLLAADAAATEARRAAIRKDRLAKAVPTAEWMKGERDRILK
KEAGVHVQQMFAASFGLGPKWEEGFRKFWDLPIDWRLMEADLPIPSYGRDYSMDLSELPDVKTQVFVEE
```

(b)  $\beta$  subunit of AC from *Rb. capsulatus* SB1003

```
MPLDREKTRSVQVLGIDAGGTMTDTFFVDANGDFVVGKAQSTPQNEALGLLESSREGLQHWGLSLEEALS
SIQTGVYSGTAMLRVQVRKGLRCLIVNAGMEDFHRMGRAIQAYLGFAYEDRIHLNTHYYDEPLVPRHL
TRGVMERIDMFGDVVIPLREETARQAAAELIAQDVEGIVISLLHSYKNPAHERRVRDIVAEELKAGKTT
PVFASTDYYPVRKETHRTNTTILEAYAAEPSRQTLRKITGAFKENGSRDFRVMATHGGTISWKAKELAR
TIVSGPIGGVIGAKYLGEVLGYKNIACSDIGGTSFDVALITQNELTIRNDPDMARLVLSLPLVAMDSVGA
GAGSFIRLDPTYKAIKLGPDAGYRVGVCWAESGIETVTSIDCHVILGYLNPDNFLGGQVKLDRQRAWDA
MKTQIADPLGLSVEDAAAGVIELLSDLRDYLRSISMISGKGYSPSSFTCFSYGGAGPVHTYGYTEGLGFED
VIVPAWAAGFSAFGCAAADFEYRYDKSLDLNIARDGSDDLKAHEARTLNDAWHELTERVLEEFELNGYTR
DQVKLQPGFRMQYRQQLNDLEIESPIPAAKTAADWDKLVAAFNDTYGRVYAASARPELGYSVTGAIMRG
MVPIPKPKIPKEPETGATPPEAAKLGTRKFYRKKKVV DARLYRMEKLLPGNRITGPAIIESDATTFFVVPD
GFETWLDGHRLFHLKEV
```

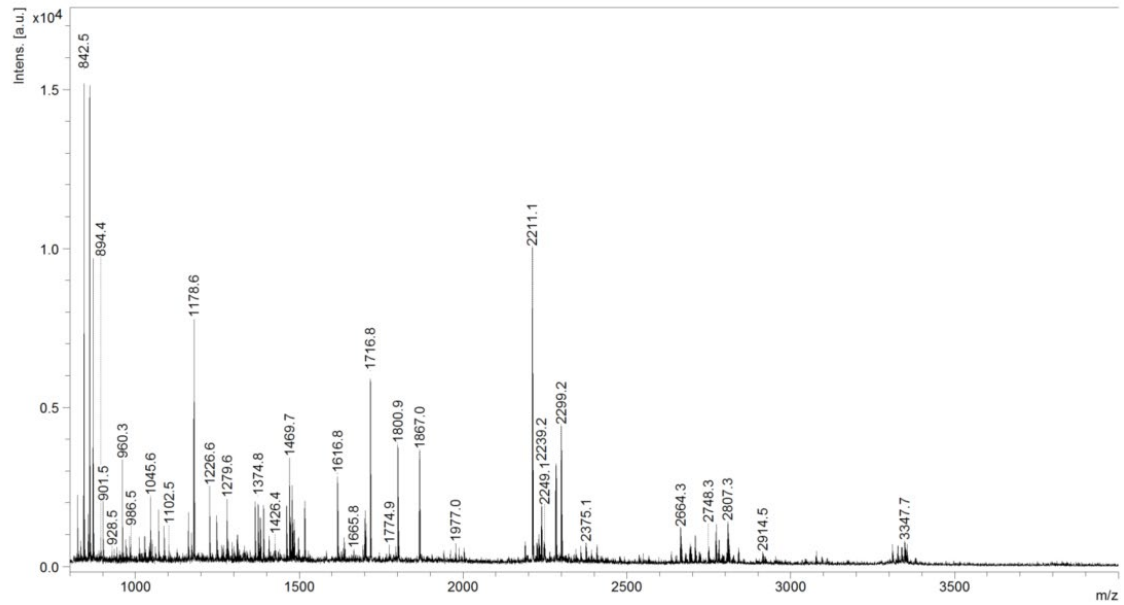
(c)  $\gamma$  subunit of AC from *Rb. capsulatus* SB1003

```
MAYTKAKIKDLVDGKIDRDTLHTMLATPKDADRVMYLEVLQDQVPWEDRIILPLGPKLYIVQRKSDHKW
VVKSHAGHEFCDWRENWKLHAVMRVRETPEAMEEIPRLMPTAGWQVIREYCCPLSGDLLDVEAPTWPY
PVIHDFEPDIDAFYSEWLGLKIPERAA
```

(d) HBDH from *Rb. capsulatus* SB1003

```
MSLKGKTAVITGSNSGIGLVARELARAGADVVLNSFTDRPEDHALAAAALGAEFGVTARYIKADMSQGAE
CRALVAQAGRCDILVNNAGIQHVAPVDQFPVEKWDAAIIA INLSSAFHTTAAALPLMRAAGWGRVNNIASA
HGLTASPFKSAVVAAKHGIVGFTKTVALETAEEPITCNAICPGYVLTPLVEAQIPDQMKVHGM DRET VIR
EVMLTRQPSKQFATVEQLGGTTVFLCAEAAAQITGTTISVDGGWTAL
```

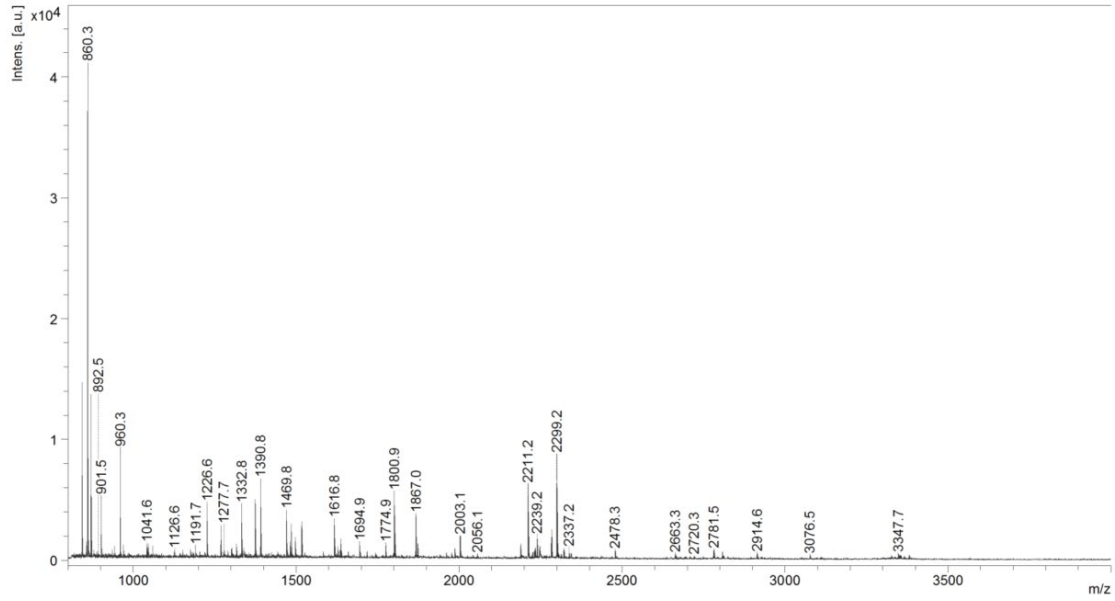
Fig. S5. The amino acid sequences of (a)  $\alpha$  subunit of AC, (b)  $\beta$  subunit of AC, (c)  $\gamma$  subunit of AC, and (d) HBDH from *Rb. capsulatus* SB1003.



M/z (Experimental value)	M/z (Calculated value)	Peak intensity	Standard error (Da)	Amino acid sequence
823.35	823.37	2186.15	-0.03	WEEGFR
894.39	894.43	805.2	-0.04	LDPEGASR
973.46	973.47	470.65	-0.01	IAGCHMIR 4: Carbamidomethyl (C) 6: Oxidation (M)
982.41	982.44	859.36	-0.03	GGCGFESLR 3: Carbamidomethyl (C)
986.54	986.57	514.7	-0.04	GERDRILK
1012.45	1012.46	857.03	-0.01	YWMLDER
1028.45	1028.45	852.12	0	YWMLDER 3: Oxidation (M)
1050.52	1050.52	747.33	0	VGENDTLFR
1070.51	1070.5	1717.12	0	DWLHESQR
1087.53	1087.52	1265.61	0.01	GGPGFGDPLDR
1161.5	1161.5	1430.22	0	FGDGYSVTCR 9: Carbamidomethyl (C)
1178.57	1178.62	7828.8	-0.05	KVGENDTLFR
1178.57	1178.56	7828.8	0.01	FAYEAVEHGR
1247.63	1247.62	1683.81	0	FWDLPIDWR
1263.61	1263.55	604.37	0.06	GTWMNPDDRR 4: Oxidation (M)
1309.76	1309.75	898.14	0	FAQSVYGVVLVK
1365.62	1365.61	1883.83	0.01	DYDLYLNMYR
1374.75	1374.68	2181.31	0.07	AVPTAEWMKGER
1381.62	1381.61	1523.76	0.01	DYDLYLNMYR 9: Oxidation (M)
1461.75	1461.74	1974.95	0.01	LMEADLPIPSYGR
1472.76	1472.73	1252.74	0.02	GADGLLAADAAATEAR
1477.75	1477.74	2473.08	0.02	LMEADLPIPSYGR 2: Oxidation (M)
1665.81	1665.81	412.52	0.01	EAGVHVQQMFAASFK 9: Oxidation (M)
1702.85	1702.89	1426.6	-0.05	LAKAVPTAEWMKGER 11: Oxidation (M)
1702.85	1702.84	1426.6	0.01	DPGAVAADVNGGYLVER
1716.85	1716.83	6125.03	0.01	QVGFVDVPIAHDDVR
2189.21	2189.15	619.05	0.05	KEAGVHVQQMFAASFGLGPK 10: Oxidation (M)
2359.13	2359.12	411.02	0.01	VDTIMHTPSEMTIRPDGTWR 5: Oxidation (M)
2359.13	2359.12	411.02	0.01	VDTIMHTPSEMTIRPDGTWR 11: Oxidation (M)
2375.13	2375.11	544.2	0.01	VDTIMHTPSEMTIRPDGTWR 5: Oxidation (M) 11: Oxidation (M)
2771.37	2771.36	819.05	0.01	EIIAQGGDIPHGGDTPGNPVWDGLLK
2771.37	2771.34	819.05	0.03	GGPGFGDPLDRDPGAVAADVNGGYLVER

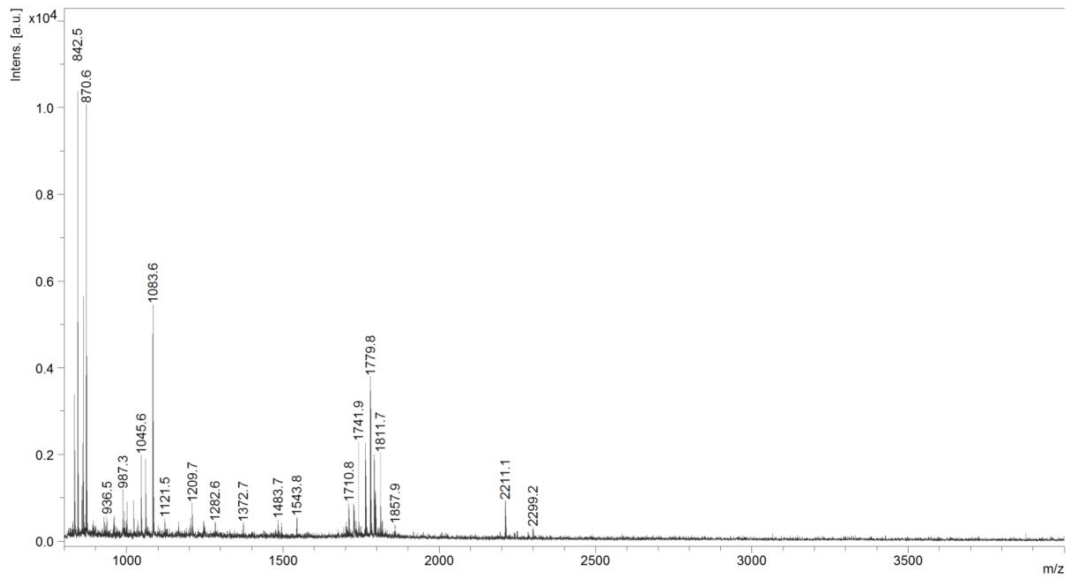
Fig. S6. The MALDI-TOF mass spectrum of the apparent molecular mass of 87.1 kDa of the electrophoretic gel as shown in Fig. 4, and the mass spectrometry peaks matched with the previously reported amino acid sequence of  $\alpha$  subunit of AC from PMF analysis.





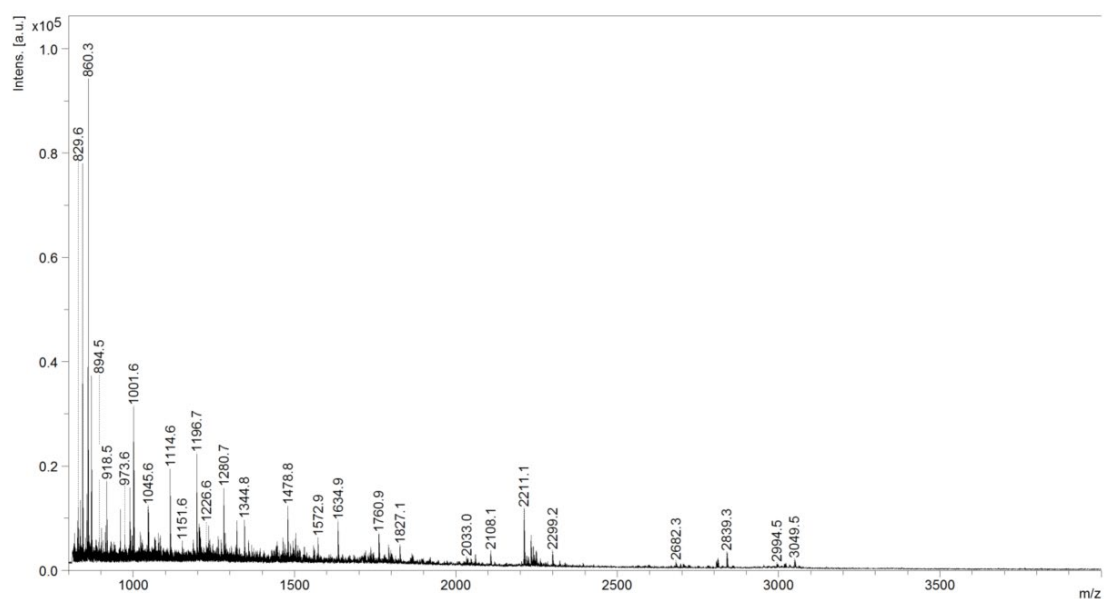
M/z (Experimental value)	M/z (Calculated value)	Peak intensity	Standard error (Da)	Amino acid sequence
901.51	901.51	5041.98	-4.77	SLDLNIAR
935.47	935.46	701.3	8.28	LGPDSAGYR
1041.58	1041.56	1400.92	13.85	YLGEVLGYK
1045.59	1045.54	1098.81	42.35	DIVAELEK
1226.64	1226.62	4748.74	22.29	LVAAFNDTYGR
1268.78	1268.76	2927.46	21.19	TIVSGPIGGVIGAK
1301.73	1301.69	887.47	29.3	DIVAELEKAGK
1374.77	1374.74	5015.07	17.77	IDMFGDVVIPLR
1390.77	1390.74	6458.55	21.46	IDMFGDVVIPLR 3: Oxidation (M)
1469.76	1469.73	4202.75	19.08	VLEEFELNGYTR
1480.78	1480.75	1432.78	25.05	SPELGYSVTGAIMR
1484.74	1484.71	2851.21	21.08	TLNDAWHELTER
1496.78	1496.74	1830.17	23.29	SPELGYSVTGAIMR 13: Oxidation (M)
1516.77	1516.74	3374.14	18.09	AIQAYLGFAYEDR
1616.83	1616.8	3300.2	20.4	TTPVFASTDYYPVR
1634.76	1634.74	746.83	12.25	CGLIVNAGMEDFHR 1: Carbamidomethyl (C) 9: Oxidation (M)
1636.86	1636.82	1416.62	23.86	TNTTILEYAAEPSR
1694.93	1694.9	1399.35	17.6	GQLNDLEIESPIPAK
1800.95	1800.91	5429.03	22.56	AQSTPQNEALGLLESSR
1866.99	1866.95	3570.95	21.84	IHLNTHYYDEPLVPR
1872.99	1872.95	1368.16	20.59	AGKTPVFASTDYYPVR
1961.05	1961.02	476.58	15.57	IDMFGDVVIPLREETAR
1977.05	1977.01	501.79	19.03	IDMFGDVVIPLREETAR 3: Oxidation (M)
2189.24	2189.2	1101.96	17.44	LVLSPVAMDSVAGAGSFI 10: Oxidation (M)
2321.2	2321.11	779.89	40.28	GLRCGLIVNAGMEDFHRMGR 4: Carbamidomethyl (C) 12: Oxidation (M) 18: Oxidation (M)
2781.49	2781.45	457.25	14.04	TQIADPLGLSVEDAAAGVIELLDSDLR
3076.55	3076.5	205.76	13.54	MQYRGQLNDLEIESPIPAKTAADWDK 1: Oxidation (M)

Fig. S7. The MALDI-TOF mass spectrum of the apparent molecular mass of 79.0 kDa of the electrophoretic gel as shown in Fig. 4, and the mass spectrometry peaks matched with the previously reported amino acid sequence of  $\beta$  subunit of AC from PMF analysis



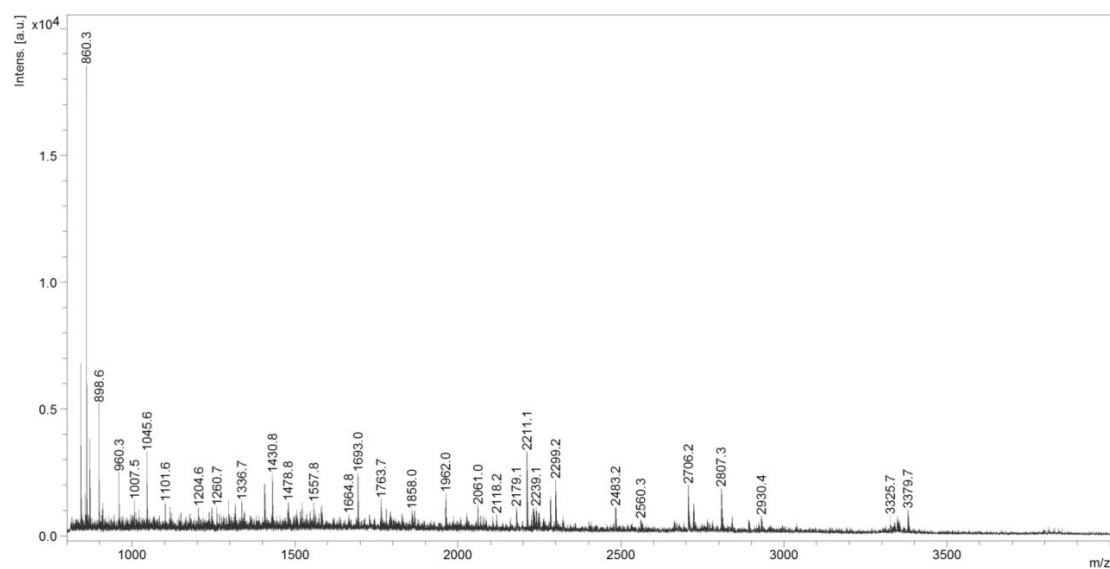
M/z (Experimental value)	M/z (Calculated value)	Peak intensity	Standard error (Da)	Amino acid sequence
850.58	850.58	4690.68	0	IILPLGPK
887.51	887.52	369.5	-0.01	IKDLVDGK
1342.75	1342.73	2381.29	0.02	LMAPTAGWQVIR
1358.74	1358.72	3639.62	0.02	LMAPTAGWQVIR 2: Oxidation (M)
1401.59	1401.58	3614.71	0.02	SHAGHEFCDWR 8: Carbamidomethyl (C)
1464.69	1464.67	887.37	0.02	ETPEAMEEIYPR
1480.69	1480.66	704.56	0.03	ETPEAMEEIYPR 6: Oxidation (M)
1611.88	1611.85	1096.06	0.03	IDRDTLHTMLATPK
1623.06	1623.04	792.01	0.02	IILPLGPKLYIVQR
1627.85	1627.85	804.76	0.01	IDRDTLHTMLATPK 9: Oxidation (M)
2183.07	2183.05	953.5	0.03	FVMYLEVLQDQVPWEDR 3: Oxidation (M)
2239.17	2239.18	1381.13	-0.01	DLVDGKIDRDTLHTMLATPK
2666.29	2666.23	272.5	0.06	SHAGHEFCDWRENWKLHAVMR 8: Carbamidomethyl (C)

Fig. S8. The MALDI-TOF mass spectrum of the apparent molecular masses of 21.3 kDa of the electrophoretic gel as shown in Fig. 4, and the mass spectrometry peaks matched with the previously reported amino acid sequence of  $\gamma$  subunit of AC from PMF analysis.



M/z (Experimental value)	M/z (Calculated value)	Peak intensity	Standard error (Da)	Amino acid sequence
1572.89	1572.87	5170.83	0.02	TAVITGSNSGIGLGVAR

Fig. S9. The MALDI-TOF mass spectrum of the apparent molecular mass of 26.8 kDa of the electrophoretic gel as shown in Fig. 5, and the mass spectrometry peaks matched with the previously reported amino acid sequence of HBDH from PMF analysis.



M/z (Experimental value)	M/z (Calculated value)	Peak intensity	Standard error (Da)	Amino acid sequence
1204.63	1204.64	710.79	0	EVMLTRQPSK 3: Oxidation (M)
1572.84	1572.87	706.81	-0.03	TAVITGSNSGIGLGVAR

Fig. S10. The MALDI-TOF mass spectrum of the apparent molecular masses of 24.6 kDa of the electrophoretic gel as shown in Fig. 5, and the mass spectrometry peaks matched with the previously reported amino acid sequence of HBDH from PMF analysis.

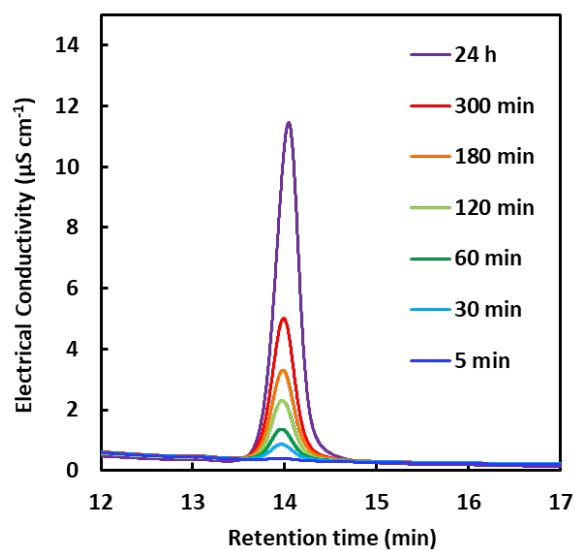


Fig. S11. Time course of the ion chromatogram for acetoacetate production with AC in the solution of  $\text{NaHCO}_3$  (50 mM), acetone (2.0 mM),  $\text{ATP}\cdot 2\text{Na}$  (5.0 mM),  $\text{MgCl}_2$  (5.0 mM) and cell extracts (0.2 mL).

As shown in Fig. S11, the peak area of acetoacetate on the ion chromatogram was increasing with the incubation time. It emphasized that AC in the cell extract catalyzed the  $\text{CO}_2$  fixation to acetone.

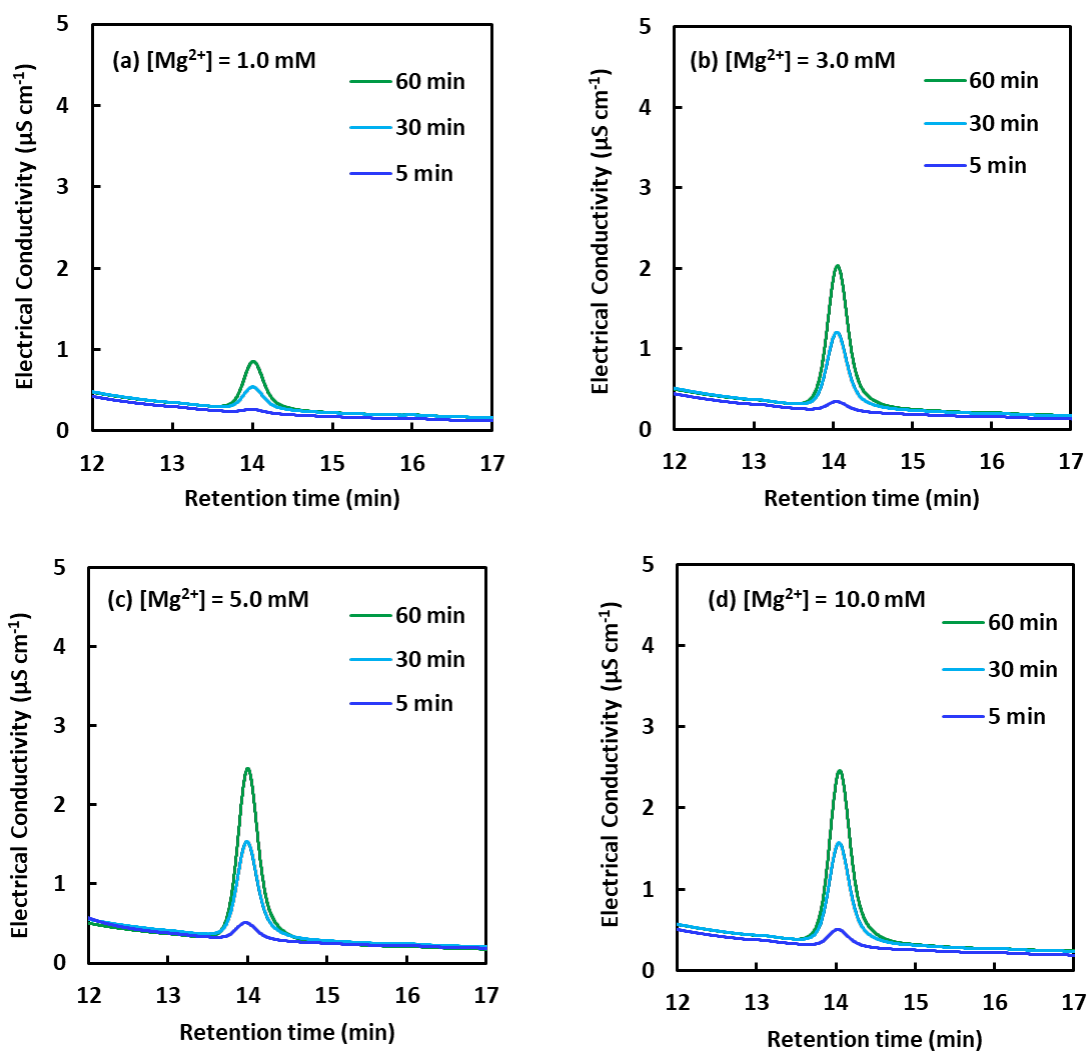


Fig. S12. Time course of the ion chromatogram for acetoacetate production with AC under various  $\text{Mg}^{2+}$  concentration in the solution of  $\text{NaHCO}_3$  (50 mM), acetone (0.5 mM),  $\text{ATP}\cdot 2\text{Na}$  (2.0 mM) and cell extracts (0.2 mL). (a)  $[\text{Mg}^{2+}] = 1.0$  mM, (b) 3.0 mM, (c) 5.0 mM, (d) 10.0 mM

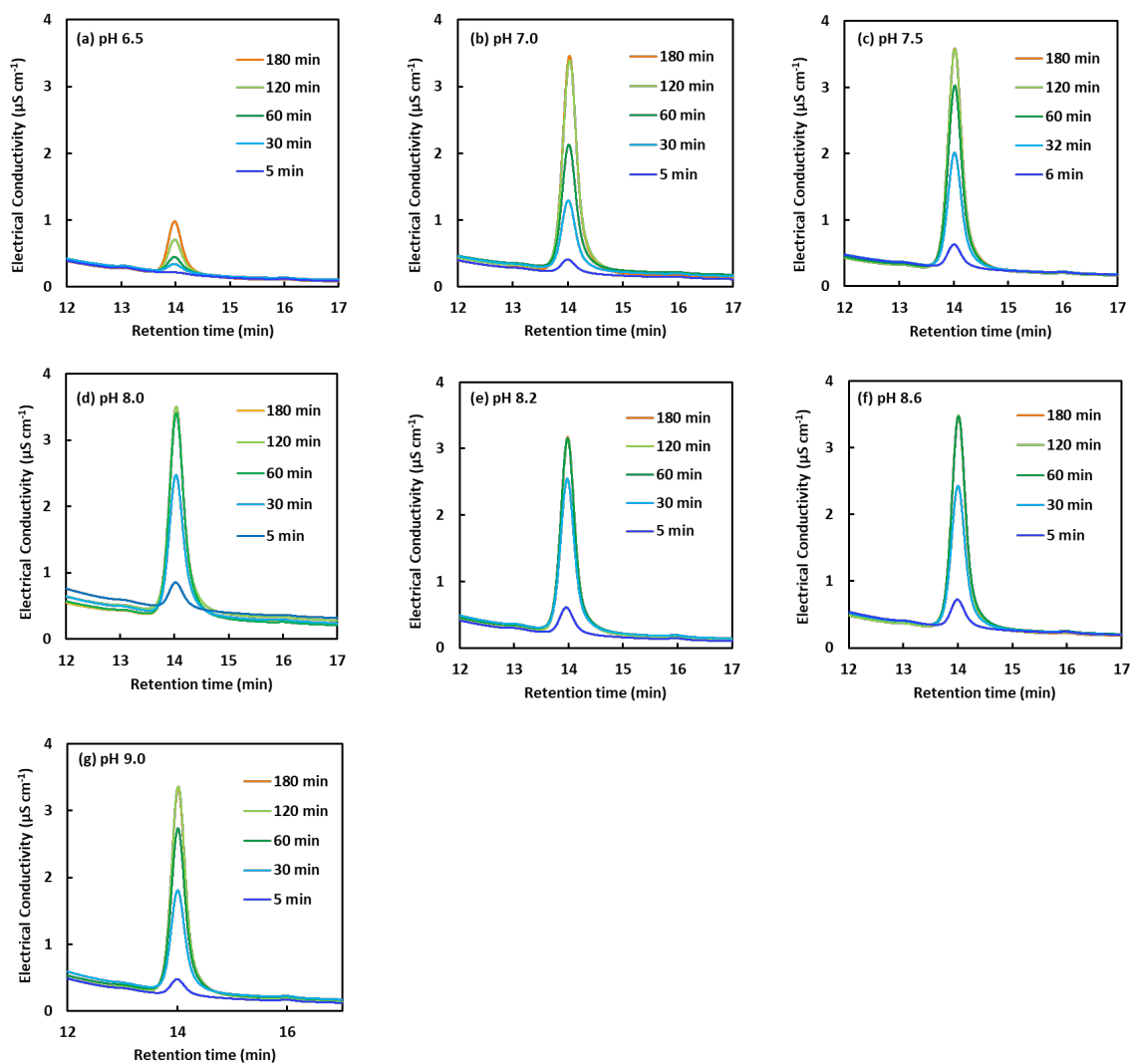


Fig. S13. Time course of the ion chromatogram for acetoacetate production with AC under various pH conditions in the solution of  $\text{NaHCO}_3$  (50 mM), acetone (0.5 mM),  $\text{ATP}\cdot 2\text{Na}$  (2.0 mM),  $\text{MgCl}_2$  (5.0 mM) and cell extracts (0.2 mL). (a) pH 6.5, (b) 7.0, (c) 7.5, (d) 8.0, (e) 8.2, (f) 8.5, (g) 9.0

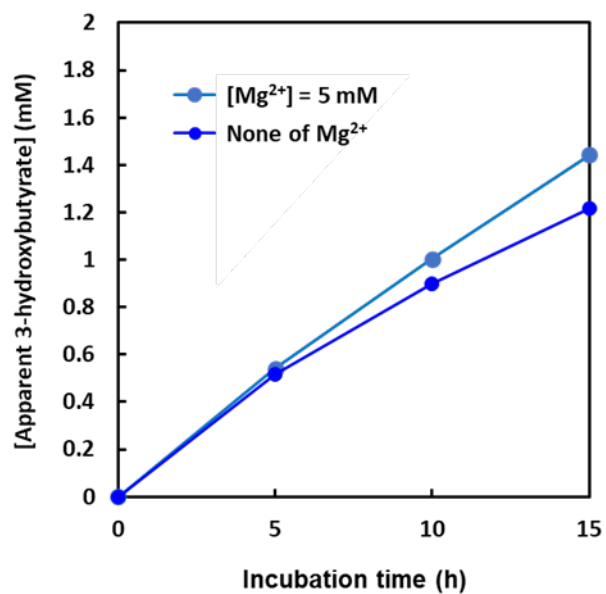


Fig. S14. Time course of the apparent  $\beta$ -hydroxybutyrate concentration in the solution of acetoacetate (2.0 mM), NADH (5.0 mM), and the cell extract (0.2 mL) with incubation time (pH7.0). The concentration of  $\text{Mg}^{2+}$ : 5 mM (●); none (●).

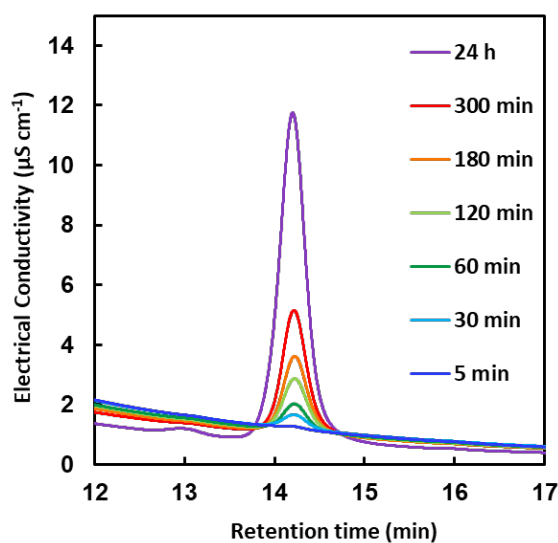


Fig. S15. Time course of the ion chromatogram for one-pot  $\beta$ -hydroxybutyrate production with AC and HBDH in the solution of  $\text{NaHCO}_3$  (50 mM), acetone (2.0 mM),  $\text{ATP}\cdot 2\text{Na}$  (5.0 mM),  $\text{MgCl}_2$  (5.0 mM), NADH (5.0 mM) and the cell extract (0.2 mL).

As shown in Fig. S15, the peak area of  $\beta$ -hydroxybutyrate on the ion chromatogram was increasing with the incubation time. Since the reaction rate of HBDH for acetoacetate reduction in the cell extract was much faster than that of AC for  $\text{CO}_2$  fixation, the peak of acetoacetate, the reaction intermediate, was not detected.

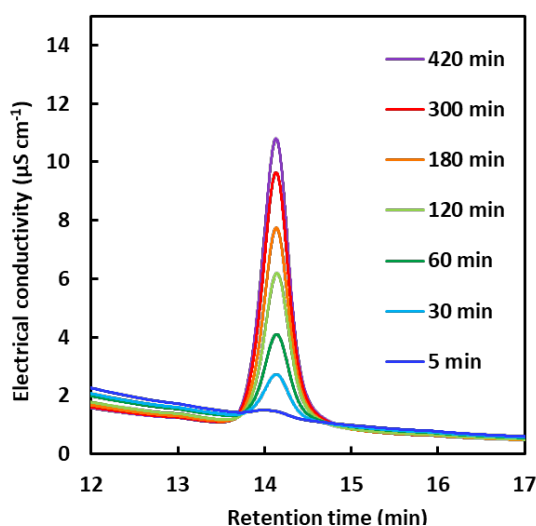


Fig. S16. Time course of the ion chromatogram for one-pot  $\beta$ -hydroxybutyrate production with AC and HBDH in the solution of  $\text{NaHCO}_3$  (50 mM), acetone (2.0 mM),  $\text{ATP}\cdot 2\text{Na}$  (5.0 mM),  $\text{MgCl}_2$  (5.0 mM), NADH (5.0 mM) and the cell extract (0.2 mL) under pH 8.2.



### Determination of stereospecificity of HBDH in the cell extract

The stereospecificity of HBDH in the cell extract was investigated by the reaction of  $\beta$ -hydroxybutyrate to acetoacetate with HBDH in the cell extract using commercial D- $\beta$ -hydroxybutyrate. The sample solution was containing of 0.2 mL cell extract (AC 0.045 U, HBDH 0.31 U), sodium D- $\beta$ -hydroxybutyrate (0.2  $\mu$ M) and NAD<sup>+</sup>(1.0 mM) in 5.0 mL of 500mM HEPES buffer (pH 7.0) at 30 °C. D- $\beta$ -hydroxybutyrate and acetoacetate were detected by the ion chromatograph system (Metrohm, Eco IC; electrical conductivity detector).

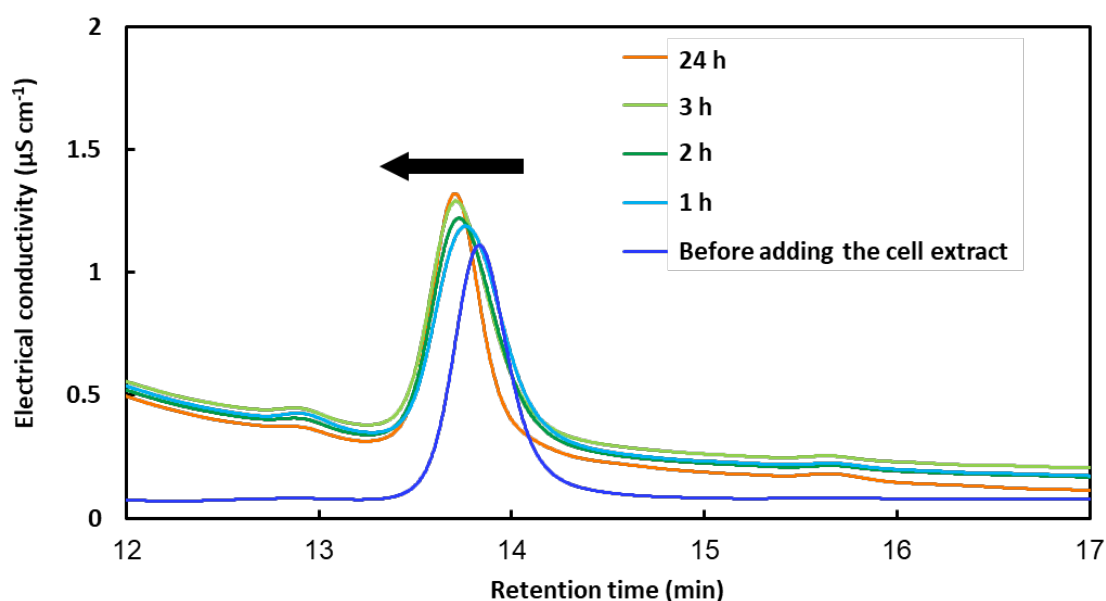


Fig. S17. Time course of the ion chromatograph for acetoacetate production with HBDH for D- $\beta$ -hydroxybutyrate oxidation in the solution of sodium D- $\beta$ -hydroxybutyrate (0.2 mM), NAD<sup>+</sup> (1 mM) and the cell extract (0.2mL; AC 0.045 U, HBDH 0.31 U).

As shown in Fig. S17, the retention time of the peak area at 13.8 min before adding the cell extract became shorter with the incubation time. Fig. S18 shows the comparison of the ion chromatogram of acetoacetate (100  $\mu$ M) and  $\beta$ -hydroxybutyrate (100  $\mu$ M). Since the retention times of acetoacetate and  $\beta$ -hydroxybutyrate are close, the production of acetoacetate from  $\beta$ -hydroxybutyrate results in a shortening retention time of  $\beta$ -hydroxybutyrate and broadening of the peak. Therefore, it was found that HBDH in the cell extract catalyzed the reaction of D- $\beta$ -hydroxybutyrate oxidation to acetoacetate as shown in Fig. S17.

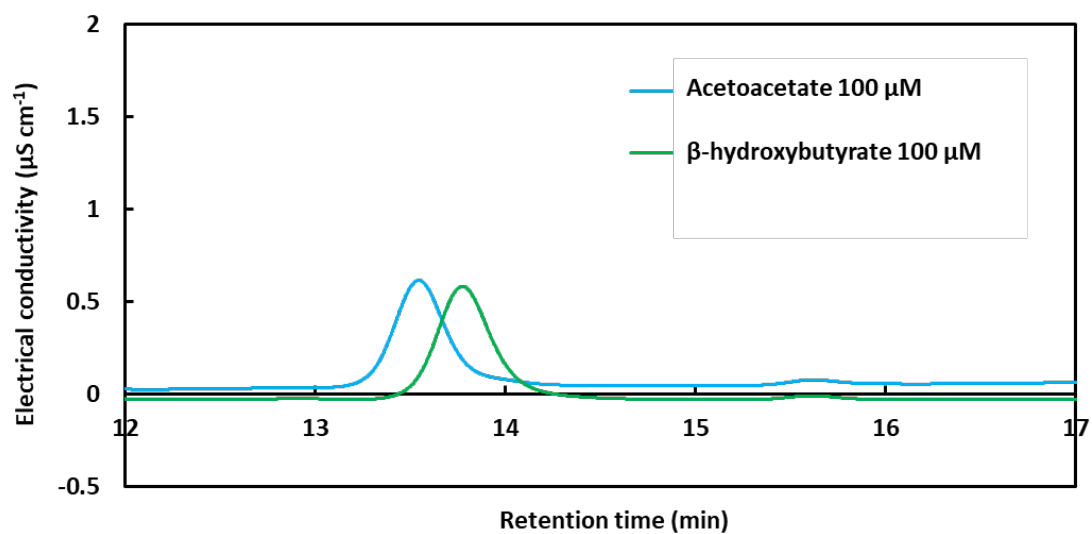


Fig. S18. Comparison of ion chromatogram of acetoacetate (100  $\mu\text{M}$ ) and  $\beta$ -hydroxybutyrate (100  $\mu\text{M}$ ) in 500 mM HEPES buffer (pH 7.0).

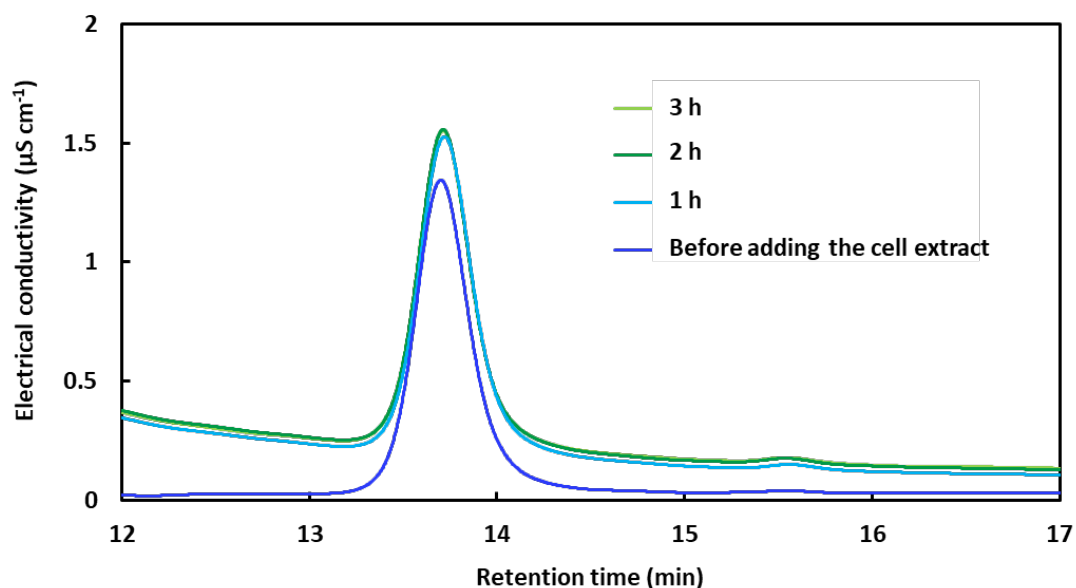


Fig. S19. Time course of the ion chromatograph for acetoacetate production with HBDH for L- $\beta$ -hydroxybutyrate oxidation in the solution of L- $\beta$ -hydroxybutyric acid (0.2 mM),  $\text{NAD}^+$  (1 mM) and the cell extract (0.2mL; AC 0.045 U, HBDH 0.31 U).

As a control experiment, HBDH in the cell extract was investigated to catalyze the  $\beta$ -hydroxybutyrate to acetoacetate using commercial L- $\beta$ -hydroxybutyrate. The sample solution was containing of 0.2 mL cell extract (AC 0.045 U, HBDH 0.31 U), L- $\beta$ -hydroxybutyric acid (0.2  $\mu\text{M}$ ) and  $\text{NAD}^+$  (1.0 mM) in 5.0 mL of 500 mM HEPES buffer (pH 7.0) at 30 °C. As shown in Fig. S19, the retention time of the peak area at 13.8 min before adding the cell extract didn't change with the incubation time. It was found that L- $\beta$ -hydroxybutyrate didn't function as a substrate for HBDH in the cell extract. This result emphasized that the substrate of HBDH in the cell extract was not L- $\beta$ -hydroxybutyrate but D- $\beta$ -hydroxybutyrate and implied that HBDH in the cell extract produced D- $\beta$ -hydroxybutyrate by the reaction of acetoacetate reduction.

### Determination of optical isomer of $\beta$ -hydroxybutyrate synthesized in a one-pot

The optical isomer of  $\beta$ -hydroxybutyrate synthesized in the one-pot was investigated by reacting  $\beta$ -hydroxybutyrate with  $\text{NAD}^+$  and commercial D-HBDH that catalyzes the oxidation of D- $\beta$ -hydroxybutyrate to acetoacetate, not that of L- $\beta$ -hydroxybutyrate to acetoacetate. The experimental procedure is as follows. First,  $\beta$ -hydroxybutyrate was synthesized in the one-pot from  $\text{CO}_2$  and acetone with the solution of acetone (2.0 mM),  $\text{NaHCO}_3$  (50 mM),  $\text{ATP}\cdot 2\text{Na}$  (5.0 mM),  $\text{MgCl}_2$  (5.0 mM),  $\text{NADH}$  (5.0 mM) and 0.2 mL cell extract (AC 0.045 U, HBDH 0.031 U) in 5.0 mL of 500 mM HEPES buffer (pH 7.0) at 30 °C.  $\beta$ -hydroxybutyrate synthesized in the 24 h one-pot reaction was heated at 95 °C for 10 minutes to inactivate the HBDH in the cell extract. Next, the heated-treated solution containing  $\beta$ -hydroxybutyrate was reacted with  $\text{NAD}^+$  and commercial D-HBDH to investigate the isomer of  $\beta$ -hydroxybutyrate synthesized in the one-pot. The sample solution was containing the 4-fold diluted solution after the one-pot reaction for 24 h,  $\text{NAD}^+$  (5.0 mM), D-HBDH (10 U) in 5.0 mL of 500 mM HEPES buffer (pH 7.0) at 30 °C.  $\beta$ -hydroxybutyrate and acetoacetate were detected by the ion chromatograph system (Metrohm, Eco IC; electrical conductivity detector).

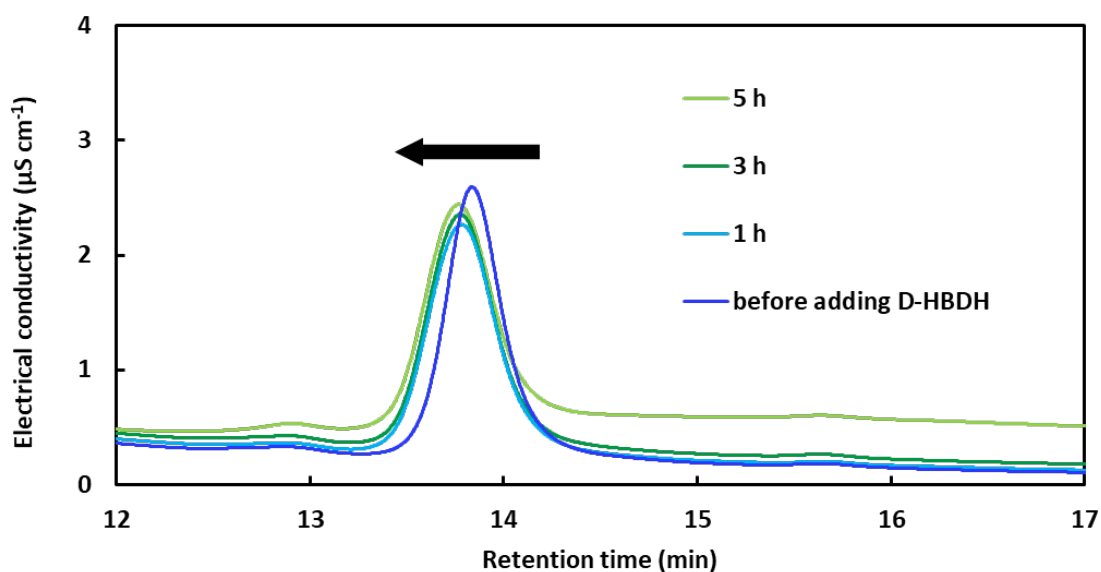


Fig. S20. Time course of ion chromatogram about acetoacetate production from  $\beta$ -hydroxybutyrate synthesized in the one-pot catalyzed by commercial D-HBDH with the solution of the solution after one-pot reaction for 24 h,  $\text{NAD}^+$  (5.0 mM) and D-HBDH (10.0 U).

As shown in Fig. S20, the retention time of the peak area at 13.8 min before adding D-HBDH became shorter with the incubation time. It indicated that  $\beta$ -hydroxybutyrate produced in the one-pot was oxidized to acetoacetate by the reaction of D-HBDH. In other words,  $\beta$ -hydroxybutyrate produced in the one-pot was concluded as D- $\beta$ -hydroxybutyrate.